

Received 17 October 2022, accepted 2 December 2022, date of publication 12 December 2022, date of current version 20 December 2022.

Digital Object Identifier 10.1109/ACCESS.2022.3228754

RESEARCH ARTICLE

Efficient Resource Allocation for Wireless-Powered MIMO-NOMA Communications

**NOOR K. BRESAM¹, (Student Member, IEEE),
WALID A. AL-HUSSAIBI^{1,2}, (Senior Member, IEEE),
FALAH H. ALI³, (Senior Member, IEEE), AND
ISRAA M. AL-MUSAWI¹, (Student Member, IEEE)**

¹Electrical Engineering Department, BETC, Southern Technical University, Basrah 42001, Iraq

²Department of Electrical Techniques, Basrah Technical Institute, Southern Technical University, Basrah 42001, Iraq

³Communications Research Group, University of Sussex, BN19QT Brighton, U.K.

Corresponding authors: Walid A. Al-Hussaibi (alhussaibi@stu.edu.iq) and Falah H. Ali (f.h.ali@sussex.ac.uk)


ABSTRACT Wireless-powered communication (WPC) is a promising technology for varied smart network applications in the industrial, commercial, and security sectors. It employs a large number of connected low-powered user equipments (UEs) in which the harvested energy from electromagnetic radiations is used for signal transmission. However, efficient resource allocation schemes are still required to optimize the performance of WPC networks over limited power and spectrum environments. In this paper, a new approach of wireless-powered multiple-input multiple-output non-orthogonal multiple access (WP-MIMO-NOMA) is designed by employing harvest-then-transmit protocol with joint time-split and power control (TS-PC) techniques to optimize the network performance and lifetime with affordable complexity. We derive the sum rate, UEs' rates, and rate region expressions based on power-domain NOMA and successive interference cancellation (SIC) decoding. An optimal joint TS-PC (OJTS-PC) scheme is proposed to maximize the network sum rate with enhanced user-fairness under constrained harvested energy level, uplink transmit power, and minimum UE's rate. Besides, a near-optimal greedy TS-PC (GTS-PC) algorithm is designed to reduce computational efforts significantly. For comparison, we derive the rate expressions for the reference WP-MIMO-OMA system based on orthogonal frequency-division multiple access (OFDMA) and time-division multiple access (TDMA). Numerical results validate the effectiveness of proposed resource allocation schemes in terms of realized sum rate, UE's rate, and user-fairness without scarifying the limited power of far UEs. This will prolong the lifetime of WPC networks operating over constrained power and bandwidth resources.

INDEX TERMS Wireless-powered communications, MIMO-NOMA, rate analysis, resource allocation, fading channels.

I. INTRODUCTION

With the vast developments of wireless technologies for 5G and beyond era, the number of connected user equipments (UEs) like smart and Internet of Things (IoT) devices, sensor nodes, and intelligent appliances is predicted to be increased in a massive scale worldwide. This will support

a smart lifestyle with important applications in varied industrial, commercial, and security sectors [1], [2], [3], [4]. To achieve this ultimate target, great research efforts have been conducted by the academia and industrial communities to address the key challenges in this field such as massive connectivity, low energy consumption, high data transmission rates, flexible multiple access schemes, wider coverage range, user-fairness, and reasonable system complexity [5], [6], [7], [8], [9].

The associate editor coordinating the review of this manuscript and approving it for publication was Lorenzo Mucchi .

A. RELATED WORKS AND MOTIVATIONS

In different wireless applications and services like IoT, sensor networks, and biomedical implants, the UEs are mostly battery-powered devices of constrained energy and may be deployed on a large-scale (hundreds to thousands) over wide-range areas. To prolong the network lifetime, this requires continuous replacement of the consumed UEs' batteries, due to data gathering, signal processing, and wireless information transfer (WIT) processes. This may potentially represent an impractical task with a high maintenance cost, particularly in rural, difficult terrain, and hazardous areas. In this context, energy harvesting (EH) from ambient radio frequency (RF) signals is considered as a promising and sustainable far-field wireless power transfer (WPT) technique for the *near-perpetual* operation of energy-efficient green networks of low-powered UEs [2], [6]. It employs simple RF to direct current (DC) rectifiers (i.e. rectennas) for charging the embedded energy storage units (batteries or super-capacitors) at the UEs. The high flexibility of WPT techniques makes the critical target of *charging anytime-anywhere* possible without the need for high investment in the infrastructure [5], [7]. However, efficient resource allocation must be realized for integrated WPT and WIT schemes in wireless-powered communication (WPC) systems operating over constrained power and bandwidth environments.

On the other hand, multiple-input multiple-output (MIMO) [10], [11], [12], [13] and non-orthogonal multiple access (NOMA) [14], [15], [16], [17], [18] schemes are considered essential parts for modern and next-generation wireless systems due to additional degree of freedom (DoF). Furthermore, the integration of MIMO-NOMA schemes can effectively support the massive increase of connected UEs and the associated data traffic over the limited spectrum and power resources [4]. In MIMO systems, the base station (BS) or the access point (AP) can be equipped with a large number of antennas to enhance the spatial multiplexing and array gains considerably. This allows simultaneous transmission of tens to hundreds of UEs without the need for extra power, time, frequency, and code resources [1], [4]. Furthermore, NOMA is considered recently by the 3rd Generation Partnership Project (3GPP) as a possible work-item for full inclusion in beyond 5G networks [15]. Based on the power-domain, NOMA utilizes different power levels for K supported UEs (two or three in practical systems) according to their associated channel gains [16]. For instance, weak users in the uplink (UL) can use low transmit power to extend the lifetime of their batteries while attaining the minimum rate and error performance targets. This has also a direct impact on satisfying the essential power difference with the strong users for efficient successive interference cancellation (SIC) decoding at the receiver. It has been shown that NOMA can significantly outperform the conventional orthogonal multiple access (OMA) techniques in terms of channel capacity without significant loss in the error rate performance [13], [14], [15], [16]. Besides, the integration of power-domain NOMA with other OMA schemes of N DoFs offers two-fold

or more user connectivity (i.e. massive connectivity of more than KN UEs) [16], [19].

The integration of RF-based WPT and WIT schemes has been investigated in the literature of multiuser WPC networks considering different time-split and/or power-split (control) strategies [20], [21], [22], [23], [24], [25]. An intensive review of the contribution aspects in this important research topic is presented in [5]. In [7] and [20], the feasibility of equipping the BS with massive MIMO antenna arrays for efficient downlink (DL) WPT has been investigated over fading channel environment. It shows an extended WPT range for a given outage performance target.

The critical problem of optimal resource allocation for simultaneous wireless information and power transfer (SWIPT) has been studied to maximize the energy efficiency of cellular IoT networks [2] with MIMO [1] and NOMA [3], and also for heterogeneous networks with NOMA [8]. In [21], a joint optimization scheme for power and time control during WPT and WIT phases, respectively has been presented to maximize the sum rate of secondary users in cognitive radio networks. However, this approach adopts the conventional time-division multiple access (TDMA) for WIT in the UL channel. In [22], power-splitting has been used for SWIPT-enabled DL NOMA by considering a controlled part of the BS power for WPT and the other portion for the WIT process. The presented optimization problem for joint power allocation and splitting control aims to concurrently maximize the total DL rate and EH at the users while maintaining the minimum requirement for the user rate and EH level. In [23], a joint user-pairing and power allocation algorithm has been presented for SWIPT DL network. The BS of the considered scheme employs a WIT beamforming matrix for supported NOMA users and a WPT beamforming matrix for EH users concurrently. It aims to maximize the spectral efficiency of NOMA users and the energy efficiency of EH users while satisfying the quality of service (QoS), EH level, and network power consumption requirements.

On other direction, *harvest-then-transmit* (HtT) protocol has been adopted for integrated WPT and WIT techniques in WPC networks [6], [9], [24], [25]. For HtT applications, the communication time frame is divided into two parts through a controlled time-split parameter. In such a case, the BS (or AP) performs DL WPT phase at first to facilitate EH by connected UEs. Then, the UEs can exploit their harvested energy for the UL WIT phase toward the BS. In [6], [9], and [24], UL NOMA has been utilized for WPC network that employs single-antenna BS and UEs. The investigated scheme in [6] has demonstrated the tradeoff between achieved data rates and fairness of connected UEs by utilizing SIC with fixed-decoding order or time-sharing decoding (more complex) strategies. Toward this end, two QoS-based approaches have been presented: maximizing the minimum rate of supported users (i.e. symmetric rates), and maximizing the system sum rate while improving the minimum individual user rate (i.e. non-symmetric rates). The presented results have revealed that NOMA with time-sharing offers enhanced

system performance compared with the reference OMA represented by TDMA. In [9], the tradeoff between the achieved sum rate and user-fairness has been revealed. It has been shown that the optimal sum rate and time allocation can be achieved with user-fairness through NOMA with time-sharing and SIC process of fixed-decoding order. The obtained results outperform that of TDMA when the supported users are located at different distances from the BS. Differ than [9], the aim of the proposed power and time control scheme in [24] is to show the tradeoff between user rate and fairness. In [25], power-splitting has been utilized in the first phase for DL SWIPT (i.e. dividing the BS power into two parts for WIT and WPT). Then, the harvested energy by each UE is exploited in the second phase for UL NOMA transmission. The presented outcomes have demonstrated that the DL power-splitting and time-splitting parameters have a direct impact on the tradeoff between UL and DL ergodic rates.

B. AIMS AND CONTRIBUTIONS

To provide cost-effective techniques for the critical requests of 5G and beyond, this work aims to significantly improve the performance and lifetime of multiuser WPC networks over constrained power and spectrum resources. Efficient resource allocation schemes are designed for integrated WPT and WIT to maximize the system sum rate with enhanced user-fairness and affordable complexity. The key issue of user-fairness can be attained in terms of maximum equal UEs' rates (i.e. *max-min* fairness) irrespective of their channel conditions, or unequal UEs' rates (i.e. *proportional* fairness) by allowing maximum rate transmission for strong channel UEs (to maximize the sum rate) while satisfying the minimum rate request of weak channel UEs [4], [9], [24]. These approaches with the aid of NOMA are very important for alleviating the inherent *double near-far* problem in WPC networks (i.e. far UEs from the BS may get low EH levels compared with the near UEs, but must utilize more transmit power for sum rate maximization) [9], [24]. Reducing the computational efforts (complexity) is also considered to minimize the consumed power towards green WPC networks [1], [2], [4], [5], [6].

In this paper, a new approach of wireless-powered MIMO-NOMA (WP-MIMO-NOMA) networks is proposed by employing HtT protocol with joint time-split and power control (TS-PC) schemes. The BS is equipped with multiple antennas for energy transmission (ET) and to support data transmission (DT) from single-antenna UEs of constrained EH level, UL transmit power, and minimum data rate. Over the adopted time frame structure, UEs perform EH during the DL phase and then utilized the stored power in the UL phase for NOMA signal transmission. For the latter, a SIC-based receiver is considered at the BS to perform multiuser signal detection. It should be noted that the previous works in [6], [9], [24], and [25] have considered the basic network scenario of single-antenna BS. Moreover, the problem of multi-antenna and joint optimization of time-split and

UL power allocation has not been tackled. The main contributions of this paper are summarized as follows:

- A complete system design of a multiuser WP-MIMO-NOMA network over realistic channel environment (large-scale and small-scale flat Rayleigh fading) is presented. It includes the transmission time frame structure for HtT strategy, DL model for ET, and UL signal model for DT.
- We derive the sum rate and individual UE's rate expressions for the UL WP-MIMO-NOMA channel with SIC-based decoding. Besides, we present the rate region equations for two UEs scenario to show the optimal operating point that maximizes the sum rate with desired user-fairness. For completeness and comparison purposes, rate expressions are derived for the reference WP-MIMO-OMA based on orthogonal frequency-division multiple access (OFDMA) and TDMA schemes.
- Optimal joint TS-PC (OJTS-PC) scheme is proposed to maximize the sum rate with improved user-fairness under constrained EH level, UL transmit power, and minimum UE's rate. Moreover, a near-optimal greedy TS-PC (GTS-PC) algorithm is designed to reduce the computational complexity considerably. The proposed techniques have a direct impact on mitigating the inherent *double near-far* problem in WP-MIMO-NOMA communication network.
- The effectiveness of the proposed designs is validated through analysis and numerical simulations compared with the reference WP-MIMO-OMA schemes. The achieved results demonstrated valuable tradeoffs between the achieved sum rate, UE's rate, user-fairness (*proportional* or *max-min*), and complexity. This will lead to *near-perpetual* and green operation of varied WPC networks over constrained power and spectrum resources.

C. PAPER ORGANIZATION AND NOTATIONS

The rest of this paper is organized as follows: Section II presents the system design of WP-MIMO-NOMA with the adopted time frame structure, ET model, and DT model. Section III deals with the sum rate and rate region analysis of the considered system model. In Section V, rate analysis for the reference WP-MIMO-OMA systems is presented. The designed resource allocation schemes including problem formulation and proposed algorithms are provided in Section IV. Numerical results and discussion are shown in Section VI. Finally, Section VII concludes the paper.

Notations: Bold-face uppercase and lowercase letters denote matrices and vectors, respectively. Plain lowercase letters stand for scalars. $\mathcal{C}^{M \times N}$ denotes complex $M \times N$ matrix. Superscripts $[\cdot]^*$, $[\cdot]^H$, and $[\cdot]^T$ stand for complex conjugate, conjugate transposition, and transposition, respectively. $\mathbb{E}[\cdot]$ stands for the expectation operator. \mathbf{I}_M stands for $M \times M$ identity matrix. $\|\cdot\|$ stands for the Euclidean vector norm while $|\cdot|$ denotes the determinant for matrices and magnitude for vectors.

II. SYSTEM DESIGN OF WP-MIMO-NOMA NETWORK

A. SYSTEM MODEL

Consider a generalized WP-MIMO-NOMA network of K single-antenna UEs communicating with a common BS over the same time-frequency channel domains. The BS is equipped with M antennas and located at the cell center as shown in Fig. 1. The connected UEs are randomly deployed within the network cell assuming sorted distances from the BS as $d_1 < \dots < d_k < \dots < d_K$. Over normalized system bandwidth ($W = 1$), the HtT protocol is adopted for each transmission time frame of duration T which is divided between the DL and UL into two phases through controlled time-split parameter α ; $0 < \alpha < 1$. In the first phase and to facilitate ET link, a fraction αT is used in the DL by the BS to broadcast wireless power P_s towards the UEs. The remaining portion of the time frame $(1 - \alpha)T$ is assigned for the second phase to allow DT from UEs with total received power constraint P_t at the BS. In this case, the UEs utilize their harvested energy (from the first phase) for simultaneous DT in the UL through power-domain NOMA with power parameters $\{\beta_k\}_{k=1}^K$; $0 < \beta_k < 1$ where $\sum_{k=1}^K \beta_k = 1$.

For the entire transmission time frame T of ET and DT links, the UEs' channels $\mathbf{h}_k = [h_{1k} \dots h_{Mk}]^T \in \mathbb{C}^{M \times 1}$; $k = 1, \dots, K$ between each UE_k and the BS are assumed to be known at the BS, where h_{mk} ; $m = 1, \dots, M$ represents the complex gain between UE_k and m^{th} receive antenna due to large-scale path loss and small-scale fading. In this case, the composite channel model of UE_k is given as [4], [17], and [23]

$$\mathbf{h}_k = \sqrt{\mathcal{L}_k} \mathbf{g}_k; \quad k = 1, \dots, K \quad (1)$$

where $\mathbf{g}_k = [g_{1k} \dots g_{Mk}]^T \in \mathbb{C}^{M \times 1}$ is the flat Rayleigh fading channel vector whose entries g_{mk} are zero-mean unit-variance complex Gaussian coefficients between UE_k and m^{th} antenna, and $\mathcal{L}_k = d_k^{-\vartheta}$ represents the large-scale path loss of UE_k based on the distance d_k from the BS and path loss exponent ϑ of considered wireless environment.

B. ET LINK MODEL

In the DL channel (i.e. phase 1 of the time frame), the BS performs ET through emitted RF signals of average power P_s towards the UEs using the allowed time fraction αT . The aggregate EH by UE_k can be found over fixed \mathbf{h}_k as [6]

$$E_k = \mathcal{G}_S \mathcal{G}_k \eta_k \zeta_k \|\mathbf{h}_k\|^2 P_s (\alpha T) \quad (2)$$

where \mathcal{G}_S and \mathcal{G}_k are the directional antenna gains of the BS and UE_k , respectively, and η_k ; $0 < \eta_k < 1$ is the energy harvesting efficiency for receiver architecture of UE_k with ζ_k RF-to-DC conversion factor capability.

C. DT LINK MODEL

In the UL, i.e. phase 2 of time $(1 - \alpha)T$, the UEs can exploit their harvested energy during the ET link for DT over their channels (\mathbf{h}_k ; $\forall k$) using the achieved powers $\{p_k = E_k / (1 - \alpha)T\}_{k=1}^K$. The received signal model

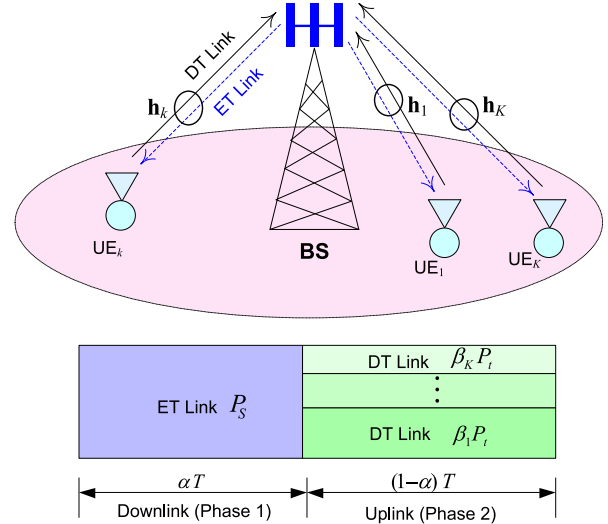


FIGURE 1. System design of WP-MIMO-NOMA network with the considered transmission time frame structure.

at M receive antennas $\mathbf{r} \in \mathbb{C}^{M \times 1}$ can be written as

$$\mathbf{r} = \sum_{k=1}^K \mathbf{h}_k \sqrt{p_k} v_k + \mathbf{n} \quad (3)$$

where v_k denotes the transmitted symbol of UE_k with $\mathbb{E}[v_k v_k^*] = 1$, and $\mathbf{n} = [n_1 \dots n_M]^T \in \mathbb{C}^{M \times 1}$ is i.i.d. complex additive white Gaussian noise (AWGN) vector with elements having zero-mean and variance σ_n^2 .

At the BS receiver and for efficient SIC-based multiuser signal detection, the received signals from all UEs should have sufficient power difference to manage the NOMA channel interference [4], [16]. Therefore, the received UEs' powers $\{\mathcal{P}_k = \beta_k P_t\}_{k=1}^K$ are controlled during the time period of DT link $(1 - \alpha)T$ based on the following total received power constraint:

$$\sum_{k=1}^K \mathcal{P}_k = \sum_{k=1}^K \beta_k P_t = \sum_{k=1}^K p_k \mathcal{L}_k. \quad (4)$$

Therefore, the transmit power of UE_k can be given by

$$p_k = \frac{\beta_k P_t}{\mathcal{L}_k}; k = 1, \dots, K. \quad (5)$$

For SIC with the assumption that $\mathcal{P}_1 > \dots > \mathcal{P}_k > \dots > \mathcal{P}_K$ due to the UEs' proximity from the BS and associated path losses, the power difference from any two successive UEs must fulfill the following condition [13], [16], [17]:

$$\left(\mathcal{P}_k - \sum_{l=k+1}^K \mathcal{P}_l \right) \geq \delta \mathcal{P}_k; k = 1, \dots, K - 1 \quad (6)$$

where the factor $\delta < 1$ is used to realize the target system error performance.

III. RATE ANALYSIS FOR WP-MIMO-NOMA

A. SUM RATE

The achievable sum rate of designed WP-MIMO-NOMA system can be given in terms of the UEs' rates as

$$R_{sum}^{NOMA} = \sum_{k=1}^K R_k \quad (7)$$

where R_k is the achievable rate of UE $_k$ based on its allowed transmit power and bounded by $R_k \geq R_0; \forall k$, and R_0 stands for the minimum UE's rate constraint.

Based on the UL sum rate capacity of multiuser MIMO channels [4], [12], [26], the achievable sum rate of received signal model (3) can be given for fixed channel realization as

$$R_{sum}^{NOMA} \leq (1 - \alpha) T \log_2 \left| \mathbf{I}_M + \sum_{k=1}^K \frac{\mathbf{h}_k p_k \mathbf{h}_k^H}{\sigma_n^2} \right|. \quad (8)$$

Using (5) of the allocated UEs' powers, the above sum rate equation can be written in terms of the power control coefficients $\{\beta_k\}_{k=1}^K$ as

$$R_{sum}^{NOMA} \leq (1 - \alpha) T \log_2 \left| \mathbf{I}_M + \gamma \sum_{k=1}^K \frac{\beta_k}{\mathcal{L}_k} \mathbf{h}_k \mathbf{h}_k^H \right| \quad (9)$$

where $\gamma = P_t / \sigma_n^2$ is the average signal-to-noise (SNR) ratio at each antenna of the BS receiver.

For SIC with fixed decoding order from UE $_1$ to UE $_K$ during each time frame, the achievable rate of UE $_k; k = 1, \dots, K - 1$ is given by

$$R_k \leq (1 - \alpha) T \log_2 \left| \mathbf{I}_M + \frac{(\gamma \beta_k / \mathcal{L}_k) \mathbf{h}_k \mathbf{h}_k^H}{\mathbf{I}_M + \gamma \sum_{i=k+1}^K \frac{\beta_i}{\mathcal{L}_i} \mathbf{h}_i \mathbf{h}_i^H} \right|. \quad (10)$$

On the other hand, the rate of UE $_K$ at the last stage of SIC without interference from other UEs can be given as

$$R_K \leq (1 - \alpha) T \log_2 \left| \mathbf{I}_M + \gamma \frac{\beta_K}{\mathcal{L}_K} \mathbf{h}_K \mathbf{h}_K^H \right|. \quad (11)$$

Thus, the ergodic sum rate for WP-MIMO-NOMA operating over randomly varying channel realizations can be found as $\mathbb{E}[R_{sum}^{NOMA}]$ while the individual ergodic UE's rate is given by $\mathbb{E}[R_k]; \forall k$.

B. RATE REGION FOR TWO UEs SCENARIO

To demonstrate the rate region of WP-MIMO-NOMA, we consider the case of two UEs scenario. For UEs' rates, R_1 and R_2 , the pentagon rate region over constant channel realization can be found based on the capacity expressions in [26] as the set of all sum rates (R_1, R_2) satisfying (9) and the following UE's rate constraints

$$R_1 = (1 - \alpha) T \log_2 \left| \mathbf{I}_M + (\gamma \beta_1 / \mathcal{L}_1) \mathbf{h}_1 \mathbf{h}_1^H \right| \quad (12)$$

$$R_2 = (1 - \alpha) T \log_2 \left| \mathbf{I}_M + (\gamma \beta_2 / \mathcal{L}_2) \mathbf{h}_2 \mathbf{h}_2^H \right|. \quad (13)$$

The maximum rate points for UE $_1$ and UE $_2$ can be achieved through (12) and (13), respectively as if the other UE is not connected. On the other hand, constraint (9) is related to the achievable sum rate when both of the UEs are communicating simultaneously with the BS. The operating corner point in the pentagon rate region can be realized using SIC to decode UE $_1$ first with the interference from UE $_2$, followed by SIC to decode the interference-free signals of UE $_2$. Thus, the optimal sum rate point that characterizes the tradeoff between the sum

rate and UEs' rates can be found using (13) and the following expression

$$R_1 = (1 - \alpha) T \log_2 \left| \mathbf{I}_M + \frac{(\gamma \beta_1 / \mathcal{L}_1) \mathbf{h}_1 \mathbf{h}_1^H}{\mathbf{I}_M + (\gamma \beta_2 / \mathcal{L}_2) \mathbf{h}_2 \mathbf{h}_2^H} \right|. \quad (14)$$

The other corner point can be found when the SIC process is reversed by decoding UE $_2$ first with interference from UE $_1$. Signals of UE $_1$ can be estimated then at the second stage of SIC without interference from UE $_2$. The achievable UEs' rates for this point can be found using (12) and the following equation

$$R_2 = (1 - \alpha) T \log_2 \left| \mathbf{I}_M + \frac{(\gamma \beta_2 / \mathcal{L}_2) \mathbf{h}_2 \mathbf{h}_2^H}{\mathbf{I}_M + (\gamma \beta_1 / \mathcal{L}_1) \mathbf{h}_1 \mathbf{h}_1^H} \right|. \quad (15)$$

IV. RATE ANALYSIS FOR WP-MIMO-OMA

In this section, and for completeness, we provide the sum rate and UEs' rates for the reference WP-MIMO-OMA over normalized bandwidth ($W = 1$). It is based on the well-known OFDMA and TDMA schemes. The main difference with the considered system model of WP-MIMO-NOMA in Section II is based on the utilized scheme for DT in the UL channel while the ET model is the same for DL. For this case, the UEs are transmitting their signals in the UL (i.e. phase 2) over orthogonal frequency/time sub-channels while the BS employs interference-free single-user detection. The transmit power for each UE is therefore given based on equal received power strategy $\{P_k = P_t / K\}_{k=1}^K$ as

$$p_k = P_t / (K \mathcal{L}_k); k = 1, \dots, K. \quad (16)$$

In this case, the critical *double near-far* problem will be realized in WP-MIMO-OMA networks since the far UEs from the BS may secure low EH levels compared with the near UEs, but require more transmit power for the sum rate maximization [9], [24].

A. OFDMA-BASED WP-MIMO-OMA

In this scheme, the UEs are allocated orthogonal frequency sub-channels of bandwidth $\{W_k\}_{k=1}^K$ and transmitting their signal simultaneously at the same time period represented by $(1 - \alpha)T$. Therefore, the sum rate for OFDMA-based WP-MIMO-OMA ($R_{sum}^{OFDMA} = \sum_{k=1}^K R_k$) of total bandwidth $W = \sum_{k=1}^K W_k$ can be written for fixed channel realization as

$$R_{sum}^{OFDMA} = (1 - \alpha) T \sum_{k=1}^K W_k \log_2 \left| \mathbf{I}_M + \frac{\gamma \mathbf{h}_k \mathbf{h}_k^H}{W \mathcal{L}_k} \right|. \quad (17)$$

Thus, the ergodic sum rate for random channel realizations can be found then as $\mathbb{E}[R_{sum}^{OFDMA}]$. Note that for rate region characterization, the rate of each UE $_k$ (R_k) depends on the allocated sub-channel bandwidth W_k . Accordingly, equal ergodic rates can be found as $R_1 = R_2 = \dots = R_K$ for the case of equal bandwidth allocation $\{W_k = W / K\}_{k=1}^K$.

B. TDMA-BASED WP-MIMO-OMA

The UEs in this scheme are allocated orthogonal time sub-channels of duration $\{T_k\}_{k=1}^K$ within the allowed portion of the time frame in phase 2 (i.e. $\sum_{k=1}^K T_k = (1 - \alpha)T$), and transmitting their signals concurrently at the same system bandwidth W . Thus, the sum rate for TDMA-based WP-MIMO-OMA ($R_{sum}^{TDMA} = \sum_{k=1}^K R_k$) can be given for fixed channel as

$$R_{sum}^{TDMA} = (1 - \alpha) T \sum_{k=1}^K T_k \log_2 \left| \mathbf{I}_M + \frac{\gamma \mathbf{h}_k \mathbf{h}_k^H}{K \mathcal{L}_k} \right|. \quad (18)$$

The ergodic sum rate for this scheme with random channel realizations can be found then as $E[R_{sum}^{TDMA}]$. From the above expression, it can be seen that the UE's rate is linearly proportional to the amount of allocated time sub-channel. Consequently, when equal time division strategy is used, i.e. $\{T_k = (1 - \alpha) T / K\}_{k=1}^K$, the rate region of connected UEs will have equal rates as $R_1 = R_2 = \dots = R_K$.

V. PROPOSED RESOURCE ALLOCATION SCHEMES

In this section, joint TS-PC schemes are proposed for WP-MIMO-NOMA to maximize the achievable sum rate with user-fairness by optimizing the EH for supported UEs and power consumption for the DT phase. The considered approaches are vital for mitigating the exhibited *double near-far* challenge. Through time-split parameter α and power control coefficients $\{\beta_k\}_{k=1}^K$, far UEs will be allowed to secure sufficient EH level for DT with low transmit power while attaining sum rate maximization target. The important trade-offs between utilized network parameters (K , α , and $\{\beta_k\}_{k=1}^K$) and achieved performance are analyzed.

A. PROBLEM FORMULATION

To provide efficient resource allocation (TS-PC) algorithms for WP-MIMO-NOMA, the following EH, UL power, and minimum rate constraints are considered:

1) EH CONSTRAINT

$$C1 : E_{min} \leq E_k \leq E_{max}; \quad k = 1, \dots, K \quad (19)$$

where this constraint is used to ensure the required EH level for wireless-powered UEs that have embedded rechargeable batteries (or super-capacitors) of maximum energy level E_{max} . On the other hand, E_{min} stands for the minimum energy level (threshold) required for signal processing and DT in the UL based on p_{min} setting over the time period $(1 - \alpha)T$. In this case, sufficient time of αT during phase 1 for the ET link is required for UE_k to satisfy the energy level condition C1 and hence, prolong the network lifetime without sacrificing the targeted network performance.

2) UL POWER CONSTRAINTS

$$C2 : P_t = \sum_{k=1}^K \underbrace{p_k \mathcal{L}_k}_{\beta_k P_t} \quad (20)$$

$$C3 : \left(\beta_k - \sum_{l=k+1}^K \beta_l \right) \geq \delta \beta_k; \quad k = 1, \dots, K - 1 \quad (21)$$

$$C4 : \underbrace{\left(\frac{E_{min}}{(1 - \alpha)T} \right)}_{p_{min}} \leq p_k \leq \underbrace{\left(\frac{E_{max}}{(1 - \alpha)T} \right)}_{p_{max}} \quad (22)$$

where C2 is used to attain the total received power condition (P_t) from all UEs, while C3 ensures the essential minimum received power difference $\delta \beta_k; k = 1, \dots, K - 1$ between any two successive UEs through power control parameters $\{\beta_k\}_{k=1}^K$. The later condition is very important to handle the inter-user interference and perform efficient SIC at the BS receiver. Constraint C4 stands for the required transmit power for each UE during DT in phase 2.

3) MINIMUM RATE CONSTRAINT

$$C5 : R_k \geq R_0; \quad k = 1, \dots, K \quad (23)$$

where C5 is used to warrant the minimum rate for each UE (particularly the weakest user, UE_K). Therefore, the upper and lower bounds of the system sum rate, R_{sum}^{NOMA} , can be written based on (9) and (23) as

$$KR_0 \leq R_{sum}^{NOMA} \leq \max_{\alpha; \{\beta_k\}_{k=1}^K} \left\{ (1 - \alpha) T \log_2 \left| \mathbf{I}_M + \gamma \sum_{k=1}^K \frac{\beta_k \mathbf{h}_k \mathbf{h}_k^H}{L_k} \right| \right\}. \quad (24)$$

For the operating corner point at the pentagon rate region with proportional fairness, the optimization problem can be formulated by maximizing the system sum rate R_{sum}^{NOMA} through (10) and (11) under C1 – C5 and for each channel realization as

$$\begin{aligned} \max_{\alpha; \{\beta_k\}_{k=1}^K} & \left[(1 - \alpha) T \left\{ \sum_{k=1}^{K-1} \log_2 \left| \mathbf{I}_M \right. \right. \right. \\ & \left. \left. + \frac{(\gamma \beta_k / L_k) \mathbf{h}_k \mathbf{h}_k^H}{\mathbf{I}_M + \gamma \sum_{i=k+1}^K \frac{\beta_i}{\mathcal{L}_i} \mathbf{h}_i \mathbf{h}_i^H} \right| \right. \\ & \left. \left. + \log_2 \left| \mathbf{I}_M + \gamma \frac{\beta_K}{\mathcal{L}_K} \mathbf{h}_K \mathbf{h}_K^H \right| \right\} \right] \\ \text{subject to : } & C1 - C5. \end{aligned} \quad (25)$$

Note that the overall sum rate maximization (25) is a mixed-integer nonlinear programming hard problem that requires an exhaustive search for the optimal joint TS-PC parameters. Moreover, closed-form solution for the optimal joint solution (α^* and $\{\beta_k^*\}_{k=1}^K$) is very difficult to be derived due to the determinants operations and co-channel interference terms. Therefore, we develop efficient optimal and near-optimal algorithms using Δ and Ω division

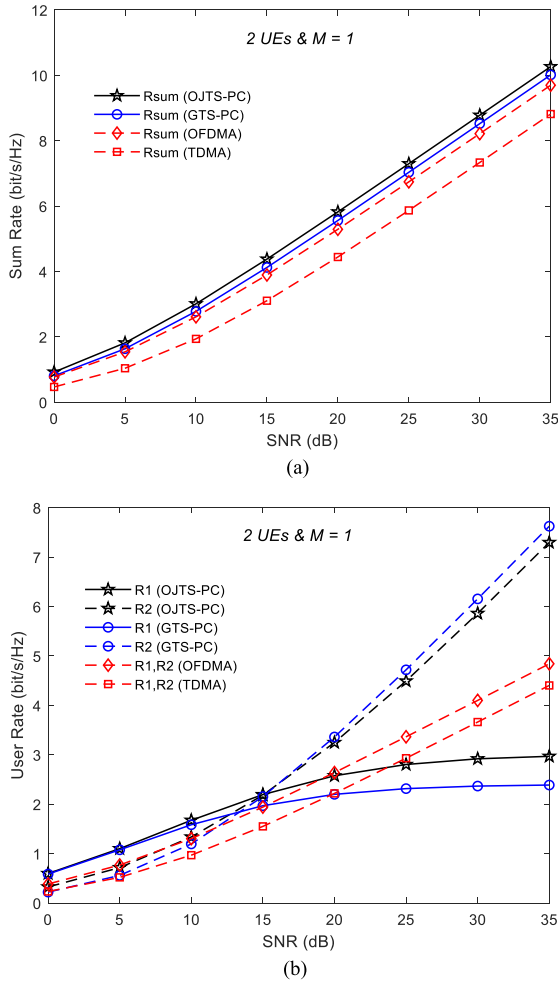


FIGURE 2. The rate performance of $K = 2$ UEs WP-MIMO-NOMA using OJTS-PC and GTS-PC algorithms and $M = 1$ as a function of SNR compared with the reference schemes: (a) Sum rate; (b) UEs' rates.

steps of equal sizes for α and $\{\beta_k\}_{k=1}^K$ parameters, respectively.

B. PROPOSED ALGORITHMS

1) ALGORITHM 1: OPTIMAL JOINT TS-PC (OJTS-PC) SCHEME

In OJTS-PC algorithm, the optimization process is performed jointly by searching for the *optimal* power coefficients using Ω division steps over all possible time-split parameter settings through Δ steps. The optimal resource parameters that maximize the sum rate (25), α^* and $\{\beta_k^*\}_{k=1}^K$, will be used for the system operating point based on the considered SIC receiver (i.e. $\{R_k^*\}_{k=1}^K$ and R_{sum}^{NOMA*}). This procedure is updated dynamically when the UEs' channels $\mathbf{h}_k; \forall k$ are changed. The pseudocode of OJTS-PC scheme is shown in Algorithm 1 with complexity efforts of $O(\Omega\Delta KM^3)$ for channel matrix manipulations that include multiplication, addition, inversion, and determinant calculations. Note that the multiplication of two $M \times M$ complex matrices requires M^3 computations while the inverse of each matrix involves Eigenvalue decomposition of $M^3/6$ calculation efforts [4].

Algorithm 1 OJTS-PC Scheme for WP-MIMO-NOMA

Input: $K, P_s, P_t, \mathcal{G}_S, \delta, T, \sigma_n^2, R_0, \Omega, \Delta, p_{min}, E_{max}$, and $\{\mathcal{G}_k, \eta_k, \zeta_k, \mathbf{h}_k\}$ for $k = 1, \dots, K$.

- 1: Define the set of UEs as $\Psi = [1, 2, \dots, K]$, sorted according to path losses in ascending order, i.e. $\mathcal{L}_1 < \mathcal{L}_2 < \dots < \mathcal{L}_K$.
- 2: Find: $\tau = 1/\Delta$ and $\mu = 1/2\Omega$.
- 3: Set $\alpha = 0$ and $R_{sum(1,1)}^{NOMA} = 0$.
- 4: **for** $n = 1$ to Δ **do**
- 5: Update $\alpha = \alpha + \tau$.
- 6: Calculate: $\{E_k\}_{k=1}^K$ in (2) and the limits E_{min} and p_{max} .
- 7: **if** $\{E_k\}_{k=1}^K$ satisfies C1 **then**
- 8: Set $\beta_1 = 0.5$.
- 9: **for** $l = 1$ to Ω **do**
- 10: Update $\beta_1 = \beta_1 + \mu$.
- 11: Calculate: $\{\beta_k\}_{k=2}^K$ based on $\sum_{k=1}^K \beta_k = 1$ and C3.
- 12: Find: $\{p_k\}_{k=1}^K$ that satisfies C2 and C4.
- 13: Calculate: $\{R_k\}_{k=1}^{K-1}$ using (10) and R_K using (11).
- 14: **if** $\{R_k\}_{k=1}^K$ satisfies C5 AND $[\sum_{k=1}^K R_k > R_{sum(n,l)}^{NOMA}]$ **then**
- 15: Update $R_{sum(n,l)}^{NOMA} = \sum_{k=1}^K R_k$, $\alpha(n,l) = \alpha$, and $\{\beta_k(n,l)\}_{k=1}^K = \{\beta_k\}_{k=1}^K$.
- 16: **end if**
- 17: **end for**
- 18: **end if**
- 19: **end for**
- 20: Choose the indices that satisfy the optimization in (25): $(n, l)^* = \arg \max_{\substack{n \in \{1, \dots, \Delta\} \\ l \in \{1, \dots, \Omega\}}} R_{sum(n,l)}^{NOMA}$.
- 21: Find the associated system parameters as: $\{R_k^*\}_{k=1}^K = \{R_k(n,l)^*\}_{k=1}^K, R_{sum}^{NOMA*} = R_{sum(n,l)^*}^{NOMA}, \alpha^* = \alpha(n,l)^*$, and $\{\beta_k^*\}_{k=1}^K = \{\beta_k(n,l)^*\}_{k=1}^K$.

Output: $\alpha^*, \{\beta_k^*\}_{k=1}^K, \{R_k^*\}_{k=1}^K, R_{sum}^{NOMA*}$.

Algorithm 2 GTS-PC Scheme for WP-MIMO-NOMA

Input: $K, P_s, P_t, \mathcal{G}_S, \delta, T, \sigma_n^2, R_0, \Delta, p_{min}, E_{max}$, and $\{\mathcal{G}_k, \eta_k, \zeta_k, \mathbf{h}_k, \beta_k^*\}$ for $k = 1, \dots, K$.

- 1: Define the set of UEs as $\Psi = [1, 2, \dots, K]$, sorted according to path losses in ascending order, i.e. $\mathcal{L}_1 < \mathcal{L}_2 < \dots < \mathcal{L}_K$.
- 2: Find: $\tau = 1/\Delta$ and $\{p_k\}_{k=1}^K$ using (5) which satisfies C2.
- 3: Set $\alpha = 0$ and $R_{sum}^{NOMA} = 0$.
- 4: **for** $n = 1$ to Δ **do**
- 5: Update $\alpha = \alpha + \tau$.
- 6: Calculate: $\{E_k\}_{k=1}^K$ in (2) and the limits E_{min} and p_{max} .
- 7: **if** $\{E_k\}_{k=1}^K$ satisfies C1 **then**
- 8: Check if the set $\{p_k\}_{k=1}^K$ satisfies C4.
- 9: Calculate: $\{R_k\}_{k=1}^{K-1}$ using (10) and R_K using (11).
- 10: **if** $\{R_k\}_{k=1}^K$ satisfies C5 AND $[\sum_{k=1}^K R_k > R_{sum}^{NOMA}]$ **then**
- 11: Update $R_{sum}^{NOMA} = \sum_{k=1}^K R_k$ and $\alpha^* = \alpha$.
- 12: **end if**
- 13: **end if**
- 14: **end for**
- 15: Find the associated system parameters as: $\{R_k^*\}_{k=1}^K = \{R_k\}_{k=1}^K, R_{sum}^{NOMA*} = R_{sum}^{NOMA}, \alpha^* = \alpha$.

Output: $\alpha^*, \{R_k^*\}_{k=1}^K, R_{sum}^{NOMA*}$.

2) ALGORITHM 2: GREEDY TS-PC (GTS-PC) SCHEME

To reduce the exhaustive search efforts for calculating the optimal parameters, a low complexity near-optimal GTS-PC scheme is proposed considering pre-defined power control

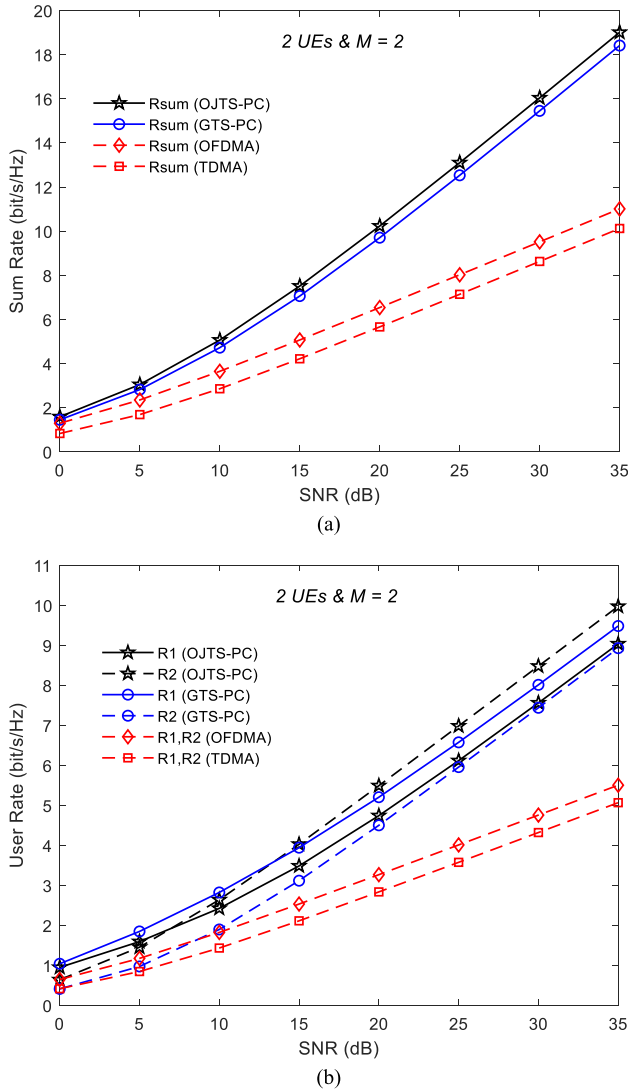


FIGURE 3. The rate performance of $K = 2$ UEs WP-MIMO-NOMA using OJTS-PC and GTS-PC algorithms and $M = 2$ as a function of SNR compared with the reference schemes: (a) Sum rate; (b) UEs' rates.

parameters based on the number of connected UEs. Based on the utilized parameters $\{\beta_k^*\}_{k=1}^K$ that satisfies $\sum_{k=1}^K \beta_k = 1$ and C3, optimal time-split parameter α^* can be selected through Δ division steps to maximize (25). The associated system rates can be found then as $\{R_k^*\}_{k=1}^K$ and R_{sum}^{NOMA*} . The considered procedure is repeated once the UEs' channels are changed. The pseudocode is shown in Algorithm 2 with considerably reduced computational efforts of $\mathcal{O}(\Delta KM^3)$.

VI. NUMERICAL RESULTS AND DISCUSSION

In this section, numerical simulations are conducted using MATLAB environment to demonstrate the effectiveness of proposed algorithms (OJTS-PC and GTS-PC) for designed WP-MIMO-NOMA network. For K UEs and M receive antennas, the achieved ergodic sum rate, UE's rate, and rate region outcomes are averaged over 10^4 channel realizations and presented in bit/s/Hz. The results are compared with reference WP-MIMO-NOMA based on OFDMA or TDMA of

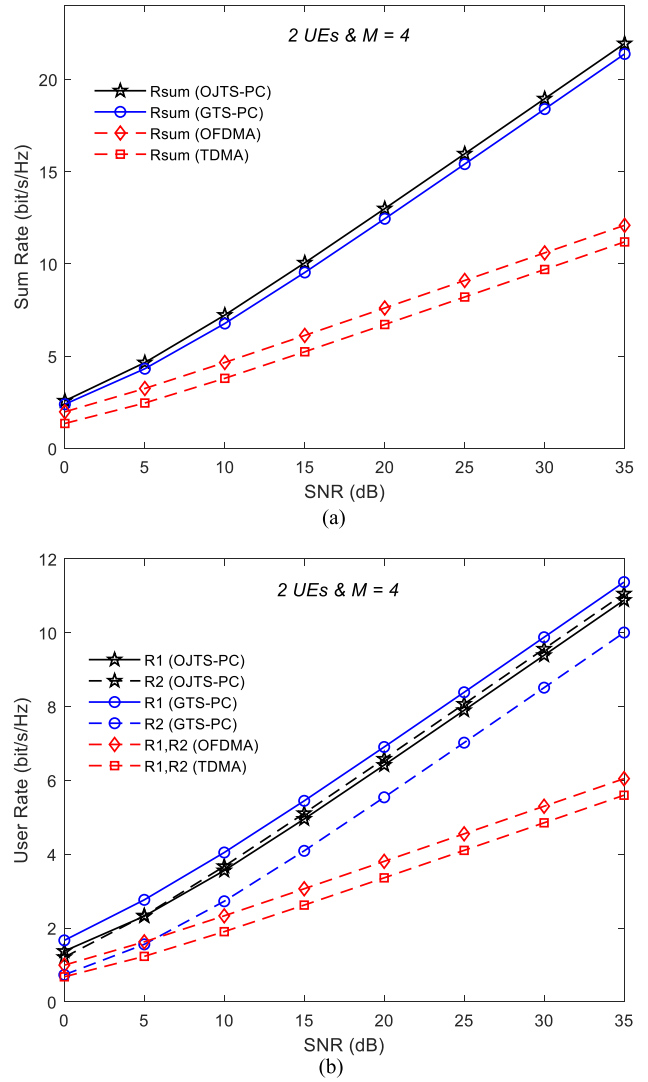


FIGURE 4. The rate performance of $K = 2$ UEs WP-MIMO-NOMA using OJTS-PC and GTS-PC algorithms and $M = 4$ as a function of SNR compared with the reference schemes: (a) Sum rate; (b) UEs' rates.

equal sub-channel divisions. The adopted simulation parameters are: network cell radius of 50m; $K = 2$ and 3 for practical NOMA [16], [25]; $M = 1 \rightarrow 4$; $P_S = K$; $P_t = 1$; $\mathcal{G}_S = 1$; $\{\mathcal{G}_k \eta_k \zeta_k = 1\}_{k=1}^K$; $T = 1$; $W = 1$; $\vartheta = 3.8$; $\delta = 0.5$; $\Delta = \Omega = 20$; and $R_0 = 0.1$ bit/s/Hz. The considered power parameters for GTS-PC scheme are $\beta_1 = 0.8$ and $\beta_2 = 0.2$ for the case of $K = 2$, while $\beta_1 = 0.7$, $\beta_2 = 0.2$, and $\beta_3 = 0.1$ are used for $K = 3$. Note that the parameters (α^* , β_k^* , E_k , and $p_k; \forall k$) are changed from one channel realization to the other. Thus, the relationship between these parameters is not presented due to the ergodic simulation environment.

For $K = 2$ UEs scenario, Figs. 2, 3, and 4 demonstrate the sum rate and UEs' rates as a function of SNR considering $M = 1, 2$, and 4, respectively. As can be seen, the sum rate of designed algorithms outperforms that of the reference schemes over the entire range of SNR, and increased significantly as the spatial diversity increased (i.e. $M \geq K$).

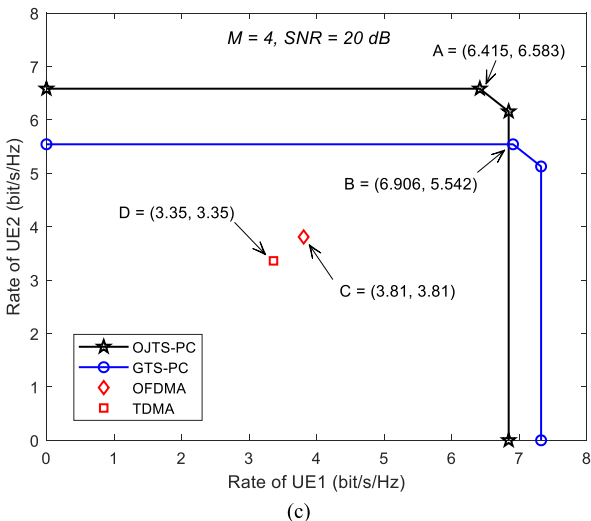
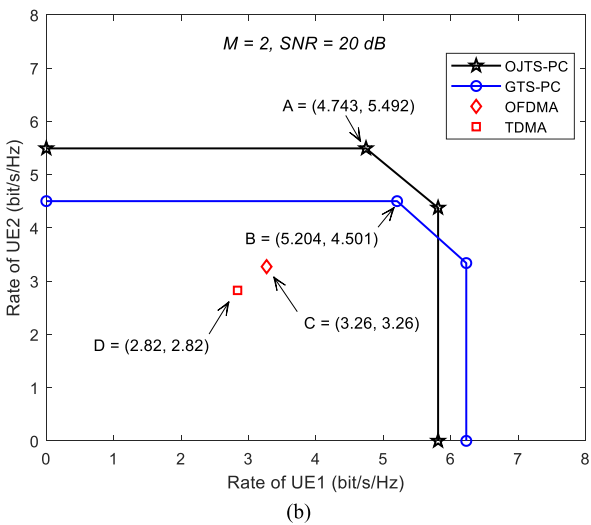
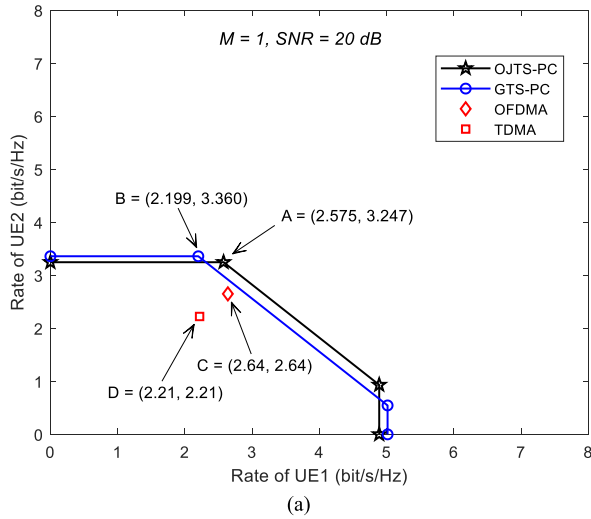


FIGURE 5. The rate region of $K = 2$ UEs WP-MIMO-NOMA using OJTS-PC and GTS-PC algorithms at SNR = 20dB compared with the reference schemes: (a) $M = 1$; (b) $M = 2$; (c) $M = 4$.

Besides, GTS-PC provides close performance (*near-optimal*) to that of OJTS-PC and outperforms the reference OFDMA

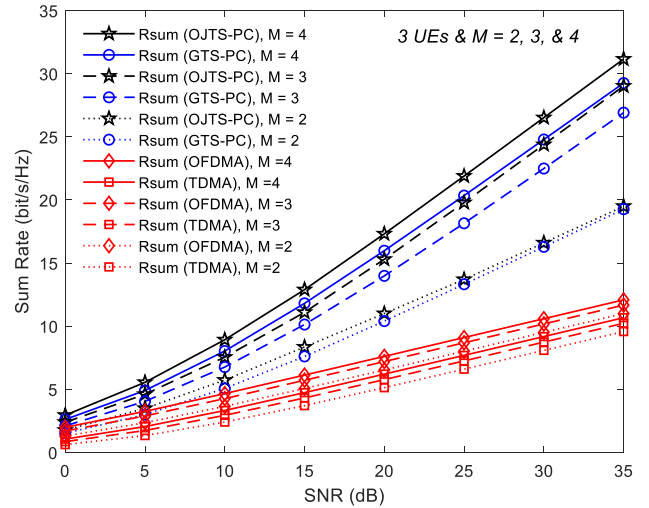


FIGURE 6. The sum rate of $K = 3$ UEs WP-MIMO-NOMA using OJTS-PC and GTS-PC algorithms and $M = 2, 3,$ and 4 as a function of SNR compared with the reference schemes.

and TDMA, respectively for any number M . Note that the sum rate gain for $M = 1$ (less than the number of UEs) in Fig. 2(a) depends completely on the power-domain of NOMA. Consequently, the achieved rate of UE₂ in Fig. 2(b) is increased as the SNR increases while UE₁ demonstrate higher performance at low to moderate SNRs, and then saturated at high SNRs owing to high inter-user interference compared with the noise power. Hence, far UE can take the advantage of SIC to achieve higher rate regardless of the low transmit power level. The equal UEs' rates point (with *max-min* fairness) is found at the intersection between R_1 and R_2 curves as 2.15 bit/s/Hz at 15 dB and 1.85 bit/s/Hz at 13 dB for OJTS-PC and GTS-PC, respectively. For $M \geq K$, both of the UEs have increased rates as the SNR increases due to spatial diversity gain. This has the effect on mitigating the *double near-far* challenge with *proportional* fairness to maximize the sum rate. The benchmark schemes (OFDMA and TDMA) of equal sub-channel divisions provide equal UEs' rates for all M values as expected. Summary of the realized outcomes at SNR of 20 dB is shown in Table 1.

Fig. 5 demonstrate the rate region of $K = 2$ UEs at target SNR of 20 dB and for $M = 1, 2,$ and 4 . Points "A", "B", "C", and "D" denote the operating rates of supported UEs using OJTS-PC, GTS-PC, OFDMA, and TDMA schemes, respectively. It can be seen clearly that the proposed OJTS-PC algorithm with SIC provides the optimal sum rate ($R_1 + R_2$) at the upper corner of the pentagon rate region and outperforms GTS-PC for all M values. This demonstrates valuable trade-offs between the sum rate, UE's rate of *proportional* fairness, and complexity. For instance in Fig. 5(b) when $M = 2$, points A = (4.743, 5.492) and B = (5.204, 4.501) are obtained for OJTS-PC and GTS-PC, respectively. The reference rate point C = (3.26, 3.26) for OFDMA has better performance than D = (2.82, 2.82) for TDMA. However, both of them are located inside the rate region with significant performance gap.

TABLE 1. Summary of rate results of $K = 2$ UEs WP-MIMO-NOMA using OJTS-PC and GTS-PC algorithms at SNR of 20 dB compared with the reference WP-MIMO-OMA system based on OFDMA and TDMA schemes.

Number of BS Antennas	Performance Measure	Rate Results of Considered Schemes in bit/s/Hz			
		WP-MIMO-NOMA		WP-MIMO-OMA	
		OJTS-PC	GTS-PC	OFDMA	TDMA
$M = 1$	<i>Sum Rate</i>	5.822	5.559	5.284	4.442
	R_1	2.575	2.199	2.642	2.221
	R_2	3.247	3.360	2.642	2.221
$M = 2$	<i>Sum Rate</i>	10.235	9.705	6.526	5.644
	R_1	4.743	5.204	3.263	2.822
	R_2	5.492	4.501	3.263	2.822
$M = 4$	<i>Sum Rate</i>	12.998	12.448	7.622	6.704
	R_1	6.415	6.906	3.811	3.352
	R_2	6.583	5.542	3.811	3.352

TABLE 2. Summary of rate results of $K = 3$ UEs WP-MIMO-NOMA using OJTS-PC and GTS-PC algorithms at SNR of 20 dB compared with the reference WP-MIMO-OMA system based on OFDMA and TDMA schemes.

Number of BS Antennas	Performance Measure	Rate Results of Considered Schemes in bit/s/Hz			
		WP-MIMO-NOMA		WP-MIMO-OMA	
		OJTS-PC	GTS-PC	OFDMA	TDMA
$M = 2$	<i>Sum Rate</i>	10.878	10.397	6.525	5.136
	R_1	3.564	3.168	2.175	1.712
	R_2	3.677	3.570	2.175	1.712
	R_3	3.637	3.659	2.175	1.712
$M = 3$	<i>Sum Rate</i>	15.297	13.980	7.179	5.766
	R_1	5.847	5.176	2.393	1.921
	R_2	5.198	4.551	2.393	1.921
	R_3	4.252	4.253	2.393	1.921
$M = 4$	<i>Sum Rate</i>	17.311	15.975	7.602	6.198
	R_1	6.829	6.172	2.534	2.066
	R_2	5.821	5.140	2.534	2.066
	R_3	4.661	4.663	2.534	2.066

In Fig. 6, the sum rate outcomes for $K = 3$ UEs scenario are shown as a function of SNR considering $M = 2, 3,$ and 4 antennas. The achieved results validate the superiority of proposed algorithms compared with the reference OFDMA and TDMA systems over the entire range of SNR and for any number of M . Moreover, the sum rate gain is increased significantly as the spatial diversity increases ($M \geq K$) which provides additional DoFs for signal detection. For instance at SNR of 20 dB and $M = 4$, optimal sum rate of 17.311 bit/s/Hz is realized by OJTS-PC while sub-optimal performance of 15.975 bit/s/Hz is obtained by GTS-PC that considerably outperforms OFDMA and TDMA schemes by about 8.3 and 9.7 bit/s/Hz, respectively. Fig. 7 demonstrates the achieved UEs' rates in this scenario as a function of SNR. For the case of $M = 2$ (i.e. insufficient spatial diversity since $M < K$), the system performance relies mainly on the power-domain. Thus, the stronger UE (i.e. UE₁) demonstrate higher performance at low to moderate SNRs, and then saturated at high SNRs due to high inter-user interference from the other UEs (UE₂ and UE₃) compared with receiver noise power.

Owing to the adopted SIC decoding procedure, UE₂ and UE₃ of low and free interference levels, respectively show increased rates as the SNR increases, regardless of their low transmit powers. This also has direct impact on attaining the limited EH based on their far distances compared with UE₁. The UEs can operate in *max-min* fairness mode with approximately 3.47 bit/s/Hz at 19.5 dB and 2.88 bit/s/Hz at 17.3 dB for OJTS-PC and GTS-PC, respectively. On the other hand with the availability of spatial diversity when $M \geq K$, all supported UEs operate in *proportional* fairness mode to maximize the system sum rate. The achieved UEs' rates are increased as the SNR increases regardless of their proximity from the BS and power conditions. The reference OFDMA and TDMA schemes of equal sub-channel division provide equal UEs' rates for all M values as expected. For example at SNR of 20 dB with $M = 4$, OJTS-PC scheme provides about 6.829, 5.821, and 4.661 bit/s/Hz for UE₁, UE₂, and UE₃, respectively compared with 2.534 and 2.066 bit/s/Hz for UEs in OFDMA and TDMA systems, respectively. It should be noted that the performance gain of the proposed

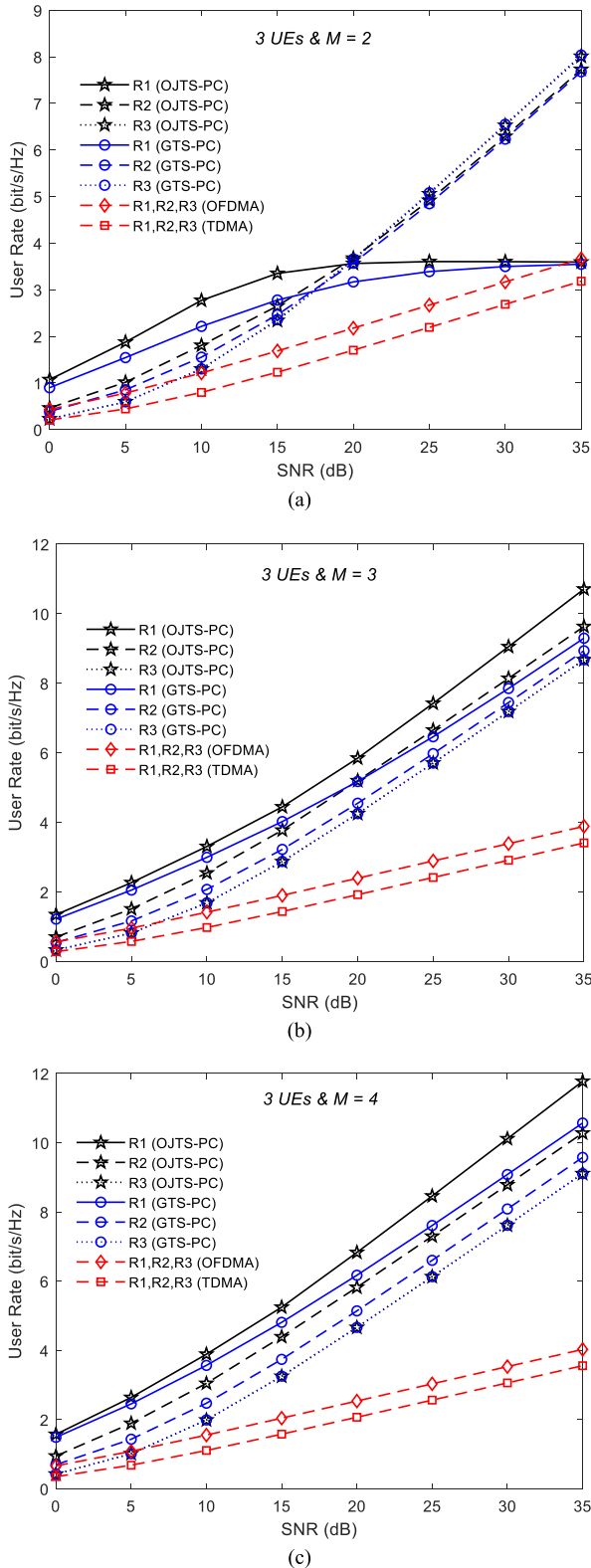


FIGURE 7. The UEs' rates of $K = 3$ UEs WP-MIMO-NOMA using OJTS-PC and GTS-PC algorithms as a function of SNR compared with the reference schemes: (a) $M = 2$; (b) $M = 3$; (c) $M = 4$.

WP-MIMO-NOMA comes at the cost of inherent inter-user interference compared with interference-free OMA schemes.

Although SIC decoding is used to mitigate this problem, it may lead to slight error performance loss. This issue is beyond the scope of this paper and will be considered in future work. Summary of the achieved results at SNR of 20 dB is presented in Table 2 to show the important system tradeoffs.

VII. CONCLUSION

In this paper, WP-MIMO-NOMA with HtT policy has been designed as a key technology for 5G and beyond to improve the network performance in terms of sum rate, UE's rate, and user-fairness with the least implementation complexity. Through adopted transmission time frame structure, supported UEs accomplish EH during the DL to perform DT in the UL phase based on controlled power-domain NOMA. For the UL channel with SIC detection, the sum rate, UEs' rates, and rate region expressions have been derived considering the key parameters for time-split and power control. Optimal and near-optimal resource allocation schemes denoted as OJTS-PC and GTS-PC, respectively are presented to maximize the sum rate with the desired user-fairness under constrained EH, UL power, and minimum UEs' rates targets. The former algorithm has computational efforts of $\mathcal{O}(\Omega\Delta KM^3)$ due to an exhaustive search for the optimal solution while the latter has much less complexity of $\mathcal{O}(\Delta KM^3)$. The achieved results validated the effectiveness of proposed algorithms compared with the reference WP-MIMO-OMA based on OFDMA and TDMA schemes. It has been shown that a significant increase in the sum rate and UE's rate can be realized with valuable tradeoffs in desired user-fairness (*max-min* or *proportional*) and complexity toward *near-perpetual* network operation.

REFERENCES

- [1] G. Femenias, J. Garcia-Morales, and F. Riera-Palou, "SWIPT-enhanced cell-free massive MIMO networks," *IEEE Trans. Commun.*, vol. 69, no. 8, pp. 5593–5607, Aug. 2021.
- [2] L. Chen, B. Hu, G. Xu, and S. Chen, "Energy-efficient power allocation and splitting for mmWave beamspace MIMO-NOMA with SWIPT," *IEEE Sensors J.*, vol. 21, no. 14, pp. 16381–16394, Jul. 2021.
- [3] H. Yang, Y. Ye, X. Chu, and M. Dong, "Resource and power allocation in SWIPT-enabled device-to-device communications based on a nonlinear energy harvesting model," *IEEE Internet Things J.*, vol. 7, no. 11, pp. 10813–10825, Nov. 2020.
- [4] W. A. Al-Hussaibi and F. H. Ali, "Efficient user clustering, receive antenna selection, and power allocation algorithms for massive MIMO-NOMA systems," *IEEE Access*, vol. 7, pp. 31865–31882, 2019.
- [5] J. Hu, K. Yang, G. Wen, and L. Hanzo, "Integrated data and energy communication network: A comprehensive survey," *IEEE Commun. Surveys Tuts.*, vol. 20, no. 4, pp. 3169–3219, 4th Quart., 2018.
- [6] P. D. Diamantoulakis, K. N. Pappi, Z. Ding, and G. K. Karagiannidis, "Wireless powered communications with non-orthogonal multiple access," *IEEE Trans. Wireless Commun.*, vol. 15, no. 12, pp. 8422–8436, Dec. 2016.
- [7] S. Kashyap, E. Björnson, and E. G. Larsson, "On the feasibility of wireless energy transfer using massive antenna arrays," *IEEE Trans. Wireless Commun.*, vol. 15, no. 5, pp. 3466–3480, May 2016.
- [8] H. Zhang, M. Feng, K. Long, G. K. Karagiannidis, V. C. M. Leung, and H. V. Poor, "Energy efficient resource management in SWIPT enabled heterogeneous networks with NOMA," *IEEE Trans. Wireless Commun.*, vol. 19, no. 2, pp. 835–845, Feb. 2020.
- [9] P. D. Diamantoulakis and G. K. Karagiannidis, "Maximizing proportional fairness in wireless powered communications," *IEEE Wireless Commun. Lett.*, vol. 6, no. 2, pp. 202–205, Apr. 2017.

- [10] A. Goldsmith, S. A. Jafar, N. Jindal, and S. Vishwanath, "Capacity limits of MIMO channels," *IEEE J. Sel. Areas Commun.*, vol. 21, no. 5, pp. 684–702, Jun. 2003.
- [11] Y. Gao, H. Vinck, and T. Kaiser, "Massive MIMO antenna selection: Switching architectures, capacity bounds, and optimal antenna selection algorithms," *IEEE Trans. Signal Process.*, vol. 66, no. 5, pp. 1346–1360, Mar. 2018.
- [12] W. A. Al-Hussaibi and F. Ali, "A closed-form approximation of correlated multiuser MIMO ergodic capacity with antenna selection and imperfect channel estimation," *IEEE Trans. Veh. Technol.*, vol. 67, no. 6, pp. 5515–5519, Jun. 2018.
- [13] W. A. Al-Hussaibi and F. H. Ali, "Performance-complexity tradeoffs of MIMO-NOMA receivers towards green wireless networks," in *Proc. IEEE 30th Annu. Int. Symp. Pers., Indoor Mobile Radio Commun. (PIMRC)*, Istanbul, Turkey, Sep. 2019, pp. 654–659.
- [14] L. Dai, B. Wang, Z. Ding, Z. Wang, S. Chen, and L. Hanzo, "A survey of non-orthogonal multiple access for 5G," *IEEE Commun. Surveys Tuts.*, vol. 20, no. 3, pp. 2294–2323, 3rd Quart., 2018.
- [15] B. Makki, K. Chitti, A. Behravan, and M.-S. Alouini, "A survey of NOMA: Current status and open research challenges," *IEEE Open J. Commun. Soc.*, vol. 1, pp. 179–189, 2020.
- [16] S. M. R. Islam, N. Avazov, O. A. Dobre, and K.-S. Kwak, "Power-domain non-orthogonal multiple access (NOMA) in 5G systems: Potentials and challenges," *IEEE Commun. Surveys Tuts.*, vol. 19, no. 2, pp. 721–742, 2nd Quart., 2017.
- [17] W. A. Al-Hussaibi, "Optimal cluster formation and power control for high connectivity wireless MIMO-NOMA applications," *Electron. Lett.*, vol. 55, no. 20, pp. 1110–1112, Oct. 2019.
- [18] I. Almusawi, W. Al-Hussaibi, and F. Ali, "Chaos-based physical layer security in NOMA networks over Rician fading channels," in *Proc. IEEE ICC*, Montreal, QC, Canada, Jun. 2021, pp. 1–6.
- [19] I. Al-Musawi, W. Al-Hussaibi, Y. H. Tahir, and F. Ali, "Chaos-based secure power-domain NOMA for wireless applications," in *Proc. 23rd Int. Symp. Wireless Pers. Multimedia Commun. (WPMC)*, Okayama, Japan, Oct. 2020, pp. 1–6.
- [20] T. A. Khan, A. Yazdan, and R. W. Heath, Jr., "Optimization of power transfer efficiency and energy efficiency for wireless-powered systems with massive MIMO," *IEEE Trans. Wireless Commun.*, vol. 17, no. 11, pp. 7159–7172, Nov. 2018.
- [21] D. Xu and Q. Li, "Joint power control and time allocation for wireless powered underlay cognitive radio networks," *IEEE Wireless Commun. Lett.*, vol. 6, no. 3, pp. 294–297, Jun. 2017.
- [22] J. Tang, Y. Yu, M. Liu, D. So, X. Zhang, Z. Li, and K.-K. Wong, "Joint power allocation and splitting control for SWIPT-enabled NOMA systems," *IEEE Trans. Wireless Commun.*, vol. 19, no. 1, pp. 120–133, Jan. 2020.
- [23] T.-V. Nguyen, V.-D. Nguyen, D. B. da Costa, and B. An, "Hybrid user pairing for spectral and energy efficiencies in multiuser MISO-NOMA networks with SWIPT," *IEEE Trans. Commun.*, vol. 68, no. 8, pp. 4874–4890, Aug. 2020.
- [24] C. Guo, B. Liao, L. Huang, Q. Li, and X. Lin, "Convexity of fairness-aware resource allocation in wireless powered communication networks," *IEEE Commun. Lett.*, vol. 20, no. 3, pp. 474–477, Mar. 2016.
- [25] S. K. Zaidi, S. F. Hasan, and X. Gui, "Evaluating the ergodic rate in SWIPT-aided hybrid NOMA," *IEEE Commun. Lett.*, vol. 22, no. 9, pp. 1870–1873, Jun. 2018.
- [26] J. G. Proakis, *Digital Communications*, 4th ed. New York, NY, USA: McGraw-Hill, 2001.



WALID A. AL-HUSSAIBI (Senior Member, IEEE) received the B.Sc. degree in electronics and communications from the University of Basrah, Iraq, in 1991, the M.Sc. degree in electronics and communications from the Jordan University of Science and Technology, Jordan, in 2000, and the Ph.D. degree in wireless and mobile communications from Sussex University, U.K., in 2011. In 2012, he joined the Southern Technical University (STU), Iraq, as a Faculty Member, where he is currently a Professor with the Department of Electrical Engineering Techniques, BETC. His research interests include 5G and beyond communications, massive MIMO, multiuser MIMO-NOMA, chaotic communications, channel modeling, capacity and performance evaluation, new modulation schemes, and multiple access techniques for future wireless systems. He is an Editor of the IEEE ACCESS and an IEEE TechRxiv Moderator.



FALAH H. ALI (Senior Member, IEEE) received the B.Sc. and M.Sc. degrees from Cardiff University, in 1984 and 1986, respectively, and the Ph.D. degree from the University of Warwick, in 1992. From 1992 to 1994, he was a Post-Doctoral Research Associate at Lancaster University. Prior to he was a Reader in Digital Communications, and a Senior Lecturer, and also a Lecturer in electronics engineering at the University of Sussex. He is a Professor of Communications Engineering at the University of Sussex. He has published more than 120 papers and has served on several international conferences technical programme committees. His current research interests include 5G/6G mobile and wireless communication systems. He is a Fellow of the IET.



NOOR K. BRESAM (Student Member, IEEE) received the B.Sc. degree in electrical engineering from the BETC, Southern Technical University (STU), Iraq, in 2016, where she is currently pursuing the Graduate degree in the field of wireless communication engineering. Her research interests include wireless-powered communications, sensor networks, 5G and beyond, mobile communications, MIMO, and MIMO-NOMA systems.



ISRAA M. AL-MUSAWI (Student Member, IEEE) received the B.Sc. and M.Sc. degrees in electrical engineering from BETC, Southern Technical University (STU), Iraq, in 2016 and 2020, respectively. She is currently a Researcher in the field of communication engineering at STU. Her research interests include wireless and mobile networks, 5G and beyond, chaos-based communications, physical layer security, and non-orthogonal multiple access.